

Supporting Information

Impact of wood combustion for secondary heating and recreational purposes on particulate air pollution concentrations in a suburb in Finland

T. Yli-Tuomi^{1*}, T. Siponen¹, R.P. Taimisto¹, M. Aurela², K. Teinilä², R. Hillamo², J. Pekkanen^{1,3}, R.O. Salonen¹, and T. Lanki¹

¹Department of Environmental Health, National Institute for Health and Welfare (THL), FI-70701, Kuopio, Finland

²Finnish Meteorological Institute, Air Quality Research, FI-00101, Helsinki, Finland

³Institute of Public Health and Clinical Nutrition, University of Eastern Finland, FI-70211, Kuopio, Finland

	Contents	Page
	Details of the chemical analysis	S2
	Details of the PMF modeling	S3
Table S1.	Meteorological conditions based on daily averages during the measurements	S5
Table S2.	Correlation coefficients (r) between the species used in the source apportionment and resolved sources	S5
Figure S1.	Locations of the central measurement site and cohort homes at a suburb Jynkkä in Kuopio	S6
Figure S2.	Temporal variation of solar radiation and oxalate to levoglucosan ratio	S6
Figure S3.	Factor contributions as a stacked column chart showing the portion of different factors to each sample	S7
Figure S4.	Five-day backward trajectories calculated at 12, 18, 00 and 06 UTC for sampling days 16.12., 20.1., 21.1., 14.2., and 13.4., which represent the five highest LRT contributions to PM _{2.5}	S7
Figure S5.	Five-day backward trajectories calculated at 12, 18, 00 and 06 UTC for sampling days 21.3., 22.3., 9.5., 10.5., and 14.5., which represent the five highest PM _{2.5} contributions from sea spray	S8
Figure S6.	Temporal variation of outdoor temperature and wood combustion related PM _{2.5} in a residential area in Kuopio	S8
Figure S7.	CPF plot for the highest 10% of the PM _{2.5} contribution from wood combustion	S9
Figure S8.	Comparison of the predicted species concentrations with the measured concentrations	S10
Figure S9.	Spearman's correlation coefficient between the central site and home outdoor location for the local component of PM _{2.5} .	S11
Figure S10.	Spearman's correlation coefficient between the central site and home outdoor location for the local component of ABS.	S11

Details of the chemical analysis

Concentrations of chlorine (Cl^-), nitrate (NO_3^-), sulfate (SO_4^{2-}), oxalate ($\text{C}_2\text{O}_4^{2-}$), sodium (Na^+), ammonium (NH_4^+) and potassium (K^+) ions were analyzed simultaneously using two Dionex ICS-2000 ion chromatography systems, one for anions and one for cations. The filter samples were extracted into 10 mL of deionized water by a short manual shaking followed by 10 min of gentle rotation. The extract was filtered through an IC Acrodisc® syringe filter (13 mm, 0.45 μm Supor® (PES) membrane, Pall Life Sciences), which was washed with deionized water freshly prior to filtering.

Organic carbon (OC) and elemental carbon (EC) were analyzed from a 1 cm² punch out of the quartz fiber filters using a thermal optical carbon analyzer (TOA; Sunset Laboratory Inc., Tigard, OR). The instrument uses a two-phase thermal method to separate OC and EC.¹ During the first phase volatile organic compounds were evaporated in four temperature steps and directed firstly to the oxidizing oven and secondly to the reduction oven. All volatilized organic compounds were converted to methane (CH_4), which is detected with a flame ionization detector (FID). Some of the OC was pyrolyzed during the first phase and was not evaporated from the filter. In the second phase pyrolyzed and elemental carbon was oxidized in two temperature steps to volatile form (method EUSAAR_1). Optical correction was made to separate pyrolyzed and elemental carbon.

Concentration of levoglucosan was analyzed using a Dionex ICS-3000 system coupled to a quadropole mass spectrometer (Dionex MSQ™).² Before the analysis, the filters were stored at +5 °C for 0-7 days, then sent to Helsinki in a cooler with ice bricks and stored at -20 °C for up to 5 months. From the Quartz fiber filters, a 1 cm² piece was punched, and it was extracted into 2.5 mL of deionized water with C-13 labeled levoglucosan as an internal standard. The extract was filtered through an IC Acrodisc® syringe filter (13 mm, 0.45 μm Supor® (PES) membrane, Pall Life Sciences), which was washed with deionized water freshly prior to filtering.

Details of the PMF modelling

Positive Matrix Factorization (PMF) is an advanced multivariate receptor modeling technique that calculates site-specific source profiles and source contributions.³ Investigators comparing results of several source apportionment methods, including PMF, concluded that the results were consistent across users and methods.⁴ One benefit of PMF compared to other methods is point-by-point scaling of the data that enables PMF to handle missing and below-detection-limit data that commonly occur during environmental measurements. The U.S. EPA's Office of Research and Development has developed a standalone graphical user interface (EPA PMF 3.0) that is freely distributed.⁵

EPA PMF 3.0 solves the general receptor model using constrained, weighted least-squares as implemented in the program ME2 (Multilinear Engine).⁶ The mathematical equation for the model is

$$x_{ij} = \sum_{p=1}^P g_{ip} f_{pj} + e_{ij} \quad \begin{pmatrix} i = 1, \dots, I \\ j = 1, \dots, J \\ p = 1, \dots, P \end{pmatrix} \quad (1)$$

where x_{ij} is the j^{th} species concentration measured in the i^{th} sample, g_{ip} is the particulate mass concentration from the p^{th} source contributing to the i^{th} sample, f_{pj} is the j^{th} species mass fraction from the p^{th} source, e_{ij} is residual associated with the j^{th} species concentration measured in the i^{th} sample, and P is the total number of independent sources.

The task of EPA PMF is to minimize the sum of squares

$$Q = \sum_{i=1}^I \sum_{j=1}^J \left(\frac{x_{ij} - \sum_{p=1}^P g_{ip} f_{pj}}{\sigma_{ij}} \right)^2 \quad (2)$$

The value σ_{ij} is the uncertainty of the measured value x_{ij} .

A pair of factor matrices (G and F) that can be transformed to another pair of matrices (G^* and F^*) with the same Q -value is said to be “rotated”. In EPA PMF3, solutions can be rotated by adjusting the parameter called F_{peak} which forces rows and columns of F and G matrices to be added and/or subtracted from each other.

PMF does not require source profiles as model inputs, but does require knowledge of source profiles and the temporal characteristics of the source contributions to interpret the factors derived from the model as air pollution sources.⁷

In this study, PMF model was run 20 times starting from different starting points using seed 1. The Q(Robust) value of the solutions varied between 873.8 and 889.3. The theoretical Q, approximated as $nm-p(n+m)$, was 800. Similar factors were produced in all 20 solutions, but solution with Q(Robust) of 877.4 was selected for further examination because it showed less rotational ambiguity based on the G-space plots between the factors than the other solutions. Q(robust) for 4 and 6 factor solutions were 1414 and 492, respectively.

Models with Fpeak strengths of 0.1, 0.2, and 0.3 yielded oblique edges on a G-space plot indicating an unrealistic rotation of factors, while strengths -0.2 and -0.1 caused only small changes in the factor compositions. Thus, the base run results are presented.

Distributions of the scaled residuals were examined. Nearly 100% of SO_4^{2-} , Na^+ , and PMCKuo were each apportioned into one factor with less than 50% of any other species. Thus, their scaled residuals varied between -1 and 1. For the other species, scaled residuals were normally distributed and varied mainly between -3 and 3, which are the reference values in PMF.⁵ Comparison of the predicted species concentrations with the measured concentrations are presented in Figure S8 in the Supplemental Information. On average, 21% of OC and 16% of Delta-C were not explained by the model. For other compounds the portion of unexplained mass was, on average, between 0 and 10%.

References

- (1) Cavalli, F.; Viana, M.; Yttri, K.E.; Genberg, J.; Putaud, J.-. Toward a standardised thermal-optical protocol for measuring atmospheric organic and elemental carbon: the EUSAAR protocol. *Atmospheric Measurement Techniques* **2010**, 3 (1), 79-89.
- (2) Saarnio, K.; Teinila, K.; Aurela, M.; Timonen, H.; Hillamo, R. High-performance anion-exchange chromatography-mass spectrometry method for determination of levoglucosan, mannosan, and galactosan in atmospheric fine particulate matter. *Analytical and Bioanalytical Chemistry* **2010**, 398 (5), 2253-2264.
- (3) Paatero, P. Least squares formulation of robust non-negative factor analysis. *Chemometrics Intellig. Lab. Syst.* **1997**, 37 (1), 23-35.
- (4) Hopke, P.; Ito, K.; Mar, T.; Christensen, W.; Eatough, D.; Henry, R.; Kim, E.; Laden, F.; Lall, R.; Larson, T., et al. PM source apportionment and health effects: 1. Intercomparison of source apportionment results. *Journal of Exposure Science and Environmental Epidemiology* **2006**, 16 (3), 275-286.
- (5) Norris, G.; Vedantham, R.; Wade, K.; Brown, S.; Prouty, J.; Foley, C. EPA Positive Matrix Factorization (PMF) 3.0: Fundamentals & User Guide. U.S. Environmental Protection Agency, Office of Research and Development: Washington, DC, **2008**.

(6) Paatero, P. The multilinear engine - A table-driven, least squares program for solving multilinear problems, including the n-way parallel factor analysis model. *Journal of Computational and Graphical Statistics* **1999**, 8 (4), 854-888.

(7) Jaekels, J.M.; Bae, M.; Schauer, J.J. Positive matrix factorization (PMF) analysis of molecular marker measurements to quantify the sources of organic aerosols. *Environ. Sci. Technol.* **2007**, 41 (16), 5763-5769.

Table S1. Meteorological conditions based on daily averages during the measurements.

Variable (unit)	mean	min	max
Temperature (°C)	-1.3	-15.3	13.7
Relative Humidity (%)	82.7	30.0	97.9
WindSpeed (m/s)	1.3	0.2	3.9
Precipitation (mm)	2.1	0.0	34.7
Solar Radiation (W/m ²)	44.0	0.0	201.3
Atmospheric pressure (kPa)	100.9	97.5	103.3

Table S2. Correlation coefficients (r) between the species used in the source apportionment and resolved sources. Correlation coefficients above 0.5 have been bolded and coefficients above 0.8 have been underlined.

	PM _{2.5}	OC	Levogluc	SO ₄ ²⁻	Na ⁺	K ⁺	PMC	NO ₂ kuo	Delta-C	BC	LRT*	TRAFFIC	ROAD-DUST	SEA-SPRAY	WOOD
PM _{2.5}											<u>0.880</u>	0.329	-0.097	-0.328	0.426
OC	0.626										0.415	0.078	0.074	-0.245	0.582
Levogluc	0.608	0.570									0.496	0.142	-0.268	-0.179	<u>0.828</u>
SO ₄ ²⁻	<u>0.890</u>	0.362	0.454								<u>0.953</u>	0.255	-0.221	-0.331	0.210
Na ⁺	-0.316	-0.240	-0.186	-0.326							-0.336	-0.206	0.185	<u>0.996</u>	-0.215
K ⁺	0.763	0.461	0.692	0.656	-0.285						0.738	0.544	-0.293	-0.305	0.556
PMC	-0.097	0.086	-0.211	-0.240	0.142	-0.190					-0.305	-0.125	<u>0.960</u>	0.100	-0.065
NO ₂ kuo	0.294	0.278	0.182	0.124	-0.115	0.273	0.331				0.056	0.664	0.383	-0.196	0.223
Delta-C	0.287	0.396	0.456	0.130	-0.140	0.328	-0.028	0.438			0.110	0.194	-0.016	-0.154	0.740
BC	0.737	0.576	0.697	0.591	-0.284	0.774	-0.062	0.509	0.593		0.618	0.494	-0.124	-0.313	0.673
LRT*	<u>0.880</u>	0.415	0.496	<u>0.953</u>	-0.336	0.738	-0.305	0.056	0.110	0.618					
TRAFFIC	0.329	0.078	0.142	0.255	-0.206	0.544	-0.125	0.664	0.194	0.494	0.249				
ROAD-DUST	-0.097	0.074	-0.268	-0.221	0.185	-0.293	<u>0.960</u>	0.383	-0.016	-0.124	-0.300	-0.177			
SEA-SPRAY	-0.328	-0.245	-0.179	-0.331	<u>0.996</u>	-0.305	0.100	-0.196	-0.154	-0.313	-0.330	-0.279	0.145		
WOOD	0.426	0.582	<u>0.828</u>	0.210	-0.215	0.556	-0.065	0.223	0.740	0.673	0.255	0.029	-0.154	-0.209	

*Long/regional range transported aerosol

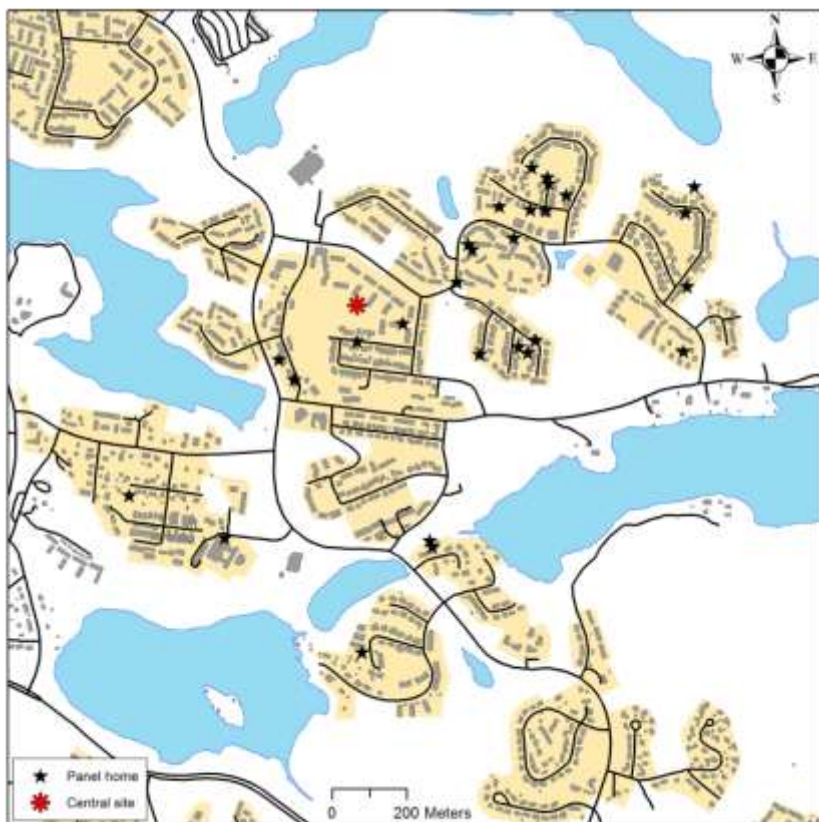


Figure S1. Locations of the central measurement site and cohort homes at a suburb Jynkkä in Kuopio. One home location is not shown and the others are presented with 50 m accuracy (random number between + and -50 has been added to both N and E coordinates) in order to prevent identification of the cohort members. Map contains data from the National Land Survey of Finland Topographic Database 01/2014.

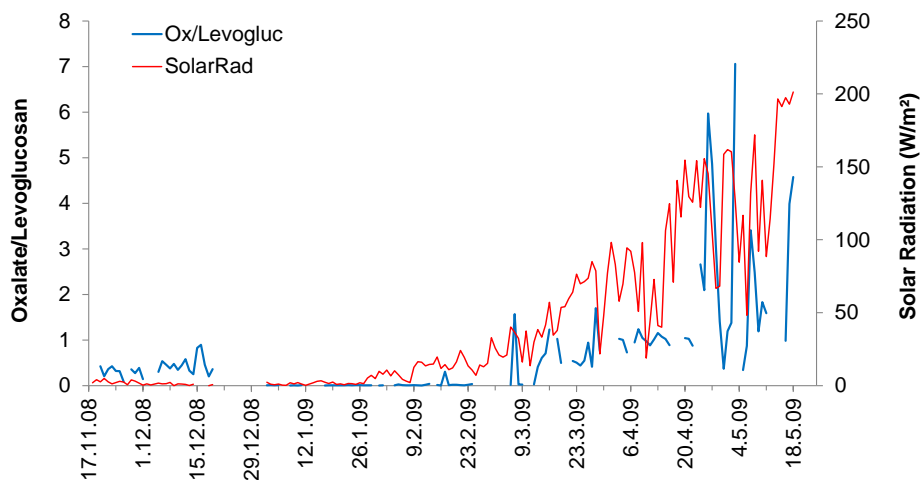


Figure S2. Temporal variation of solar radiation and oxalate to levoglucosan ratio.

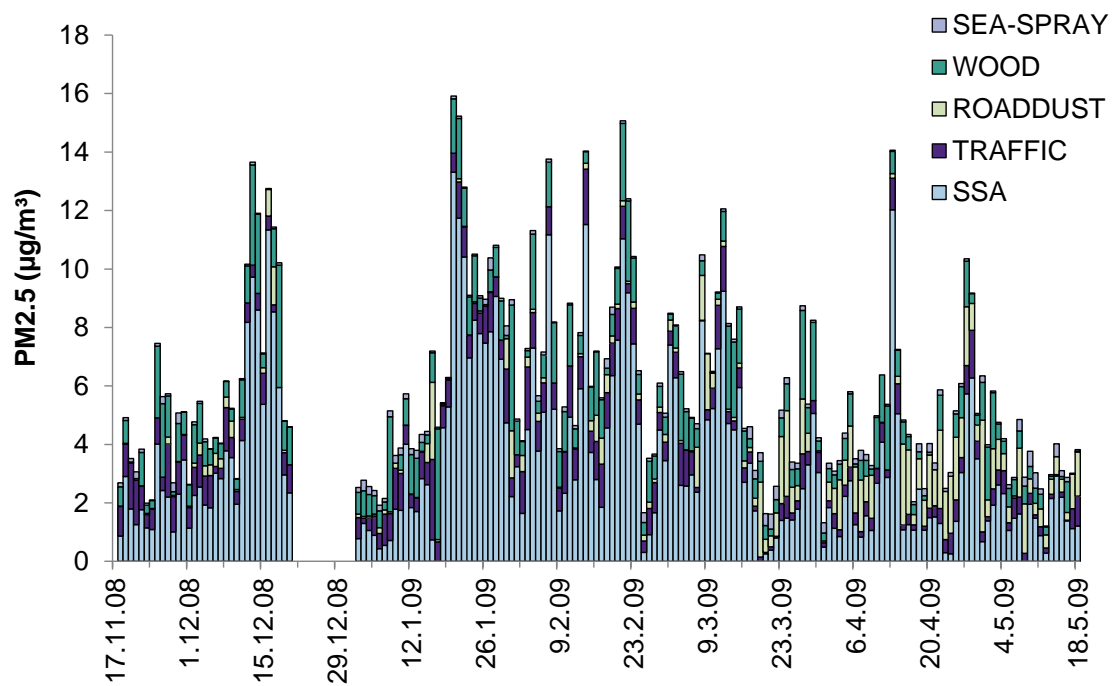


Figure S3. Factor contributions as a stacked column chart showing the portion of different factors to each sample.

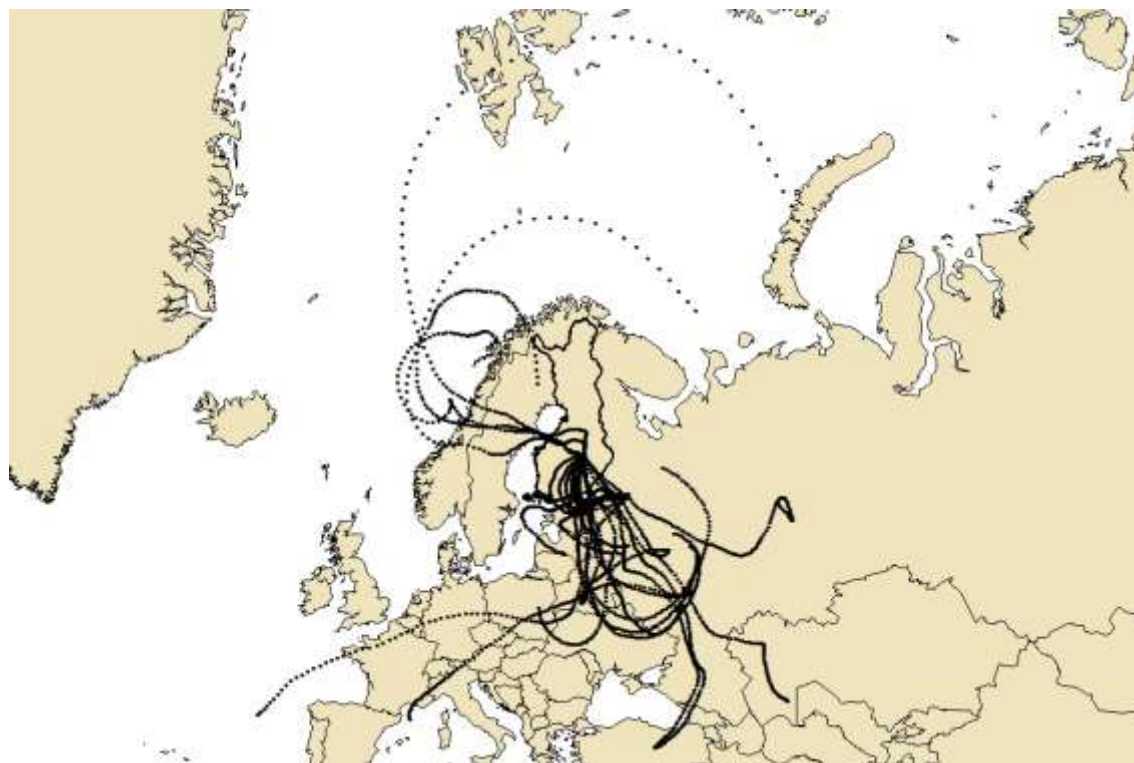


Figure S4. Five-day backward trajectories calculated at 12, 18, 00 and 06 UTC for sampling days 16.12., 20.1., 21.1., 14.2., and 13.4., which represent the five highest LRT contributions to PM_{2.5}. Used by permission. Copyright © 2013 Esri, DeLorme. All rights reserved.

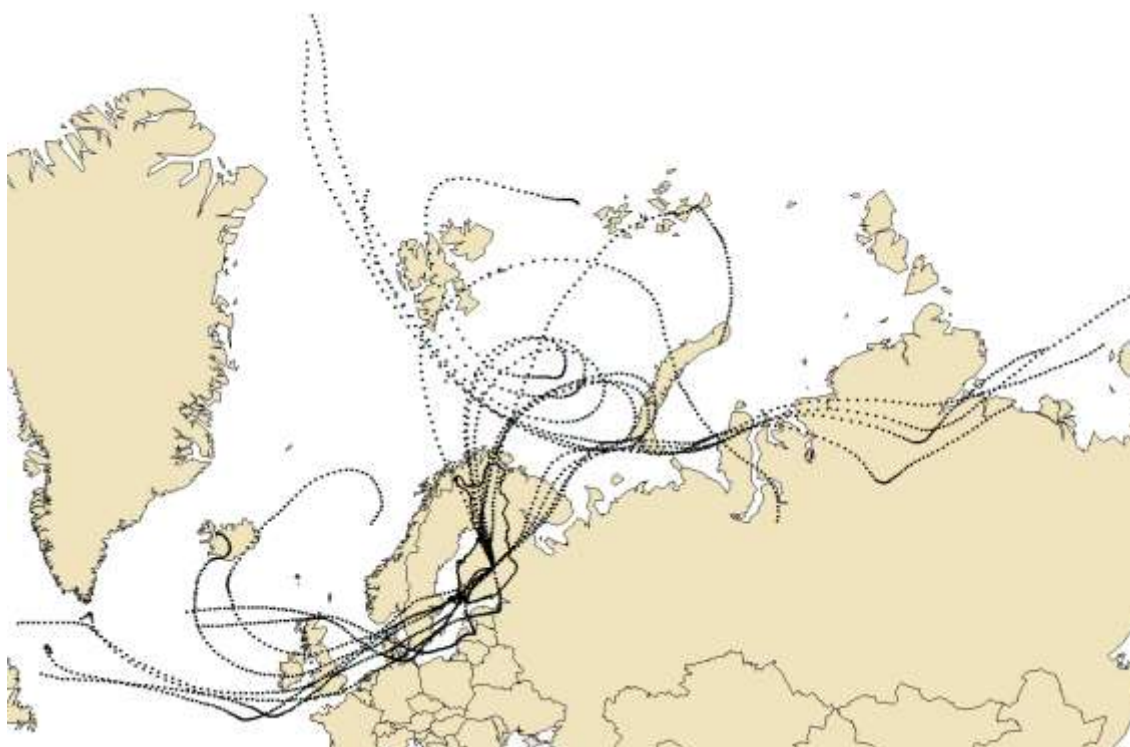


Figure S5. Five-day backward trajectories calculated at 12, 18, 00 and 06 UTC for sampling days 21.3., 22.3., 9.5., 10.5., and 14.5., which represent the five highest $PM_{2.5}$ contributions from sea spray. Used by permission. Copyright © 2013 Esri, DeLorme. All rights reserved.

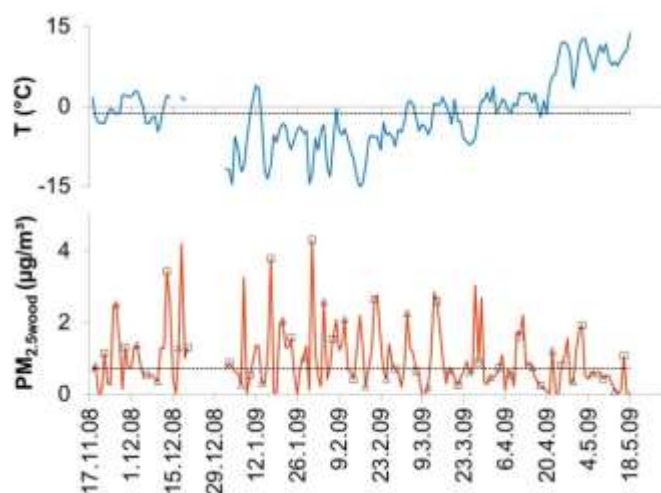


Figure S6. Temporal variation of outdoor temperature and wood combustion related $PM_{2.5}$ in a residential area in Kuopio. Triangles represent Wednesdays and squares Saturdays, which are the most common days for heating sauna. Median values are plotted with dashed lines.

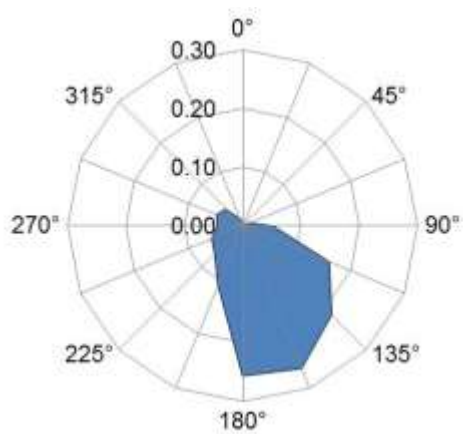


Figure S7. CPF plot for the highest 10% of the PM2.5 contribution from wood combustion.

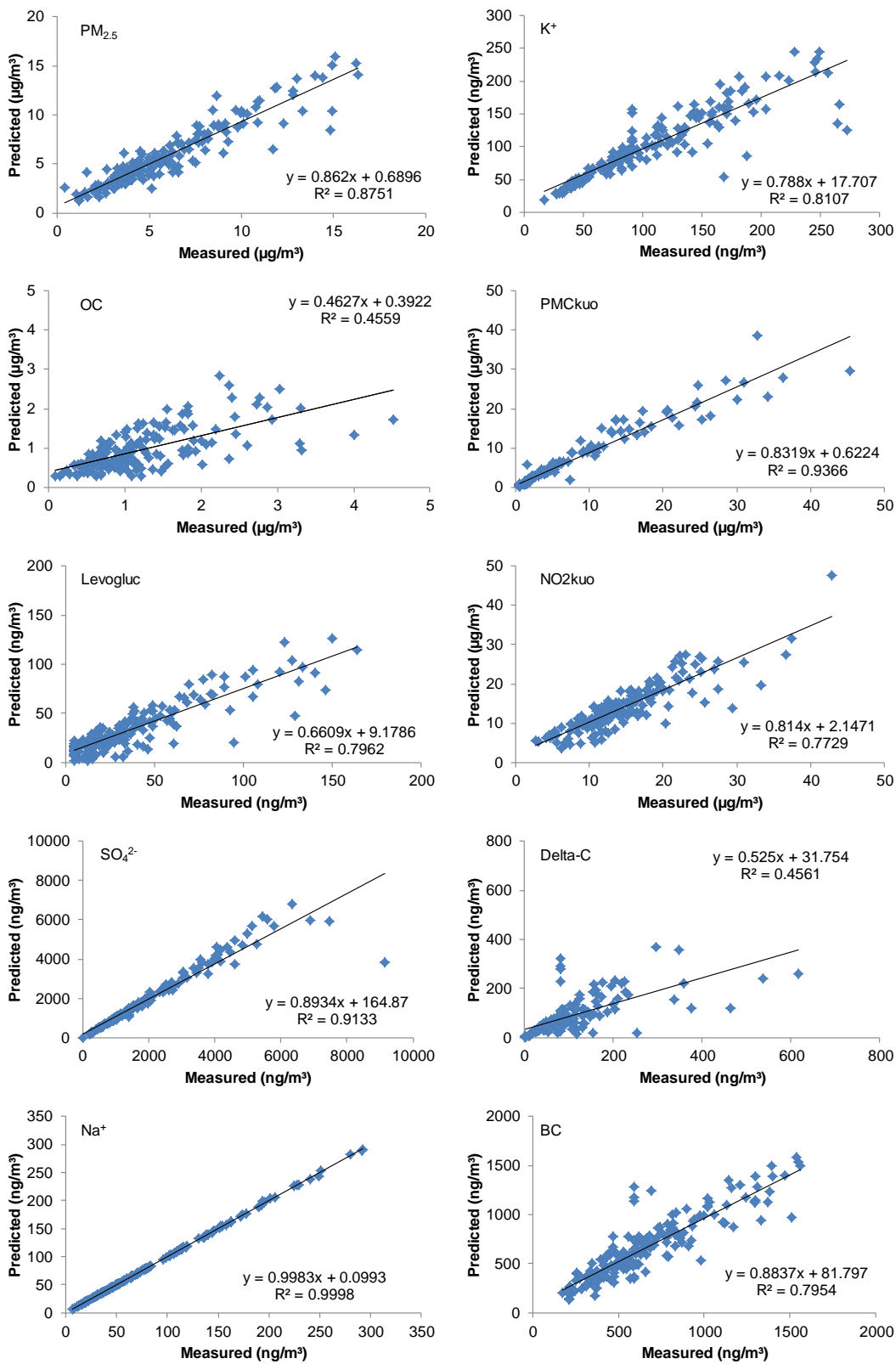


Figure S8. Comparison of the predicted species concentrations with the measured concentrations.

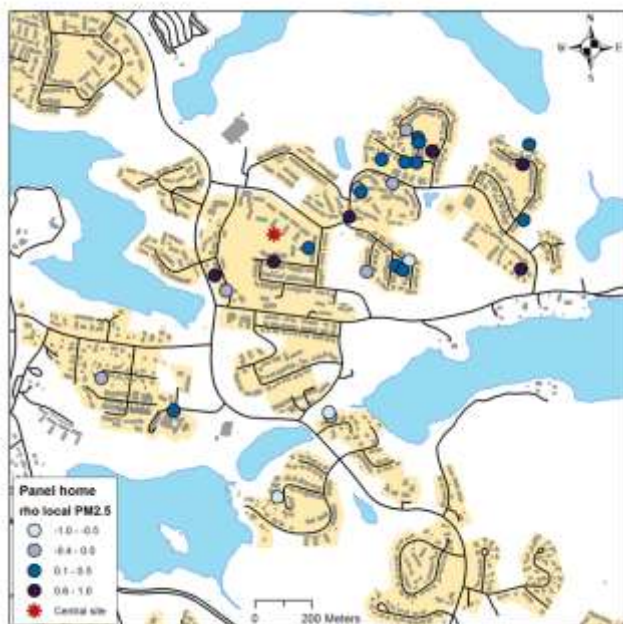


Figure S9. Spearman's correlation coefficient between the central site and home outdoor location for the local component of $PM_{2.5}$. One home location is not shown and the others are presented with 50 m accuracy (random number between + and -50 has been added to both N and E coordinates) in order to prevent identification of the panel members. Map contains data from the National Land Survey of Finland Topographic Database 01/2014.

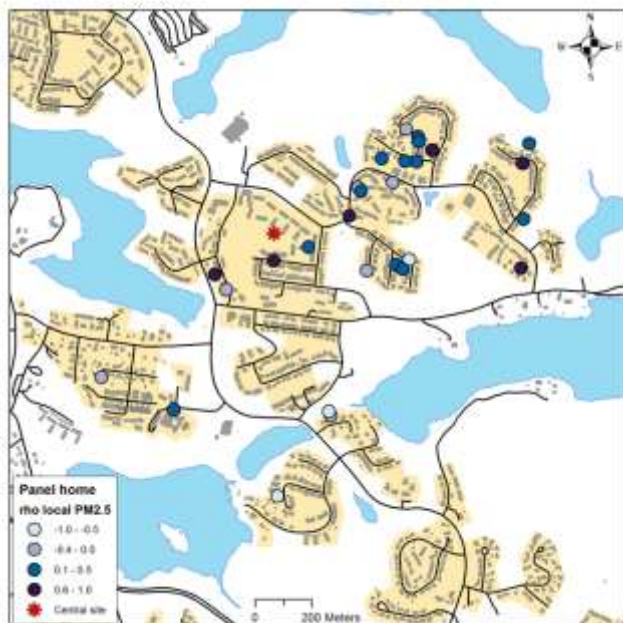


Figure S10. Spearman's correlation coefficient between the central site and home outdoor location for the local component of ABS. One home location is not shown and the others are presented with 50 m accuracy (random number between + and -50 has been added to both N and E coordinates) in order to prevent identification of the panel members. Map contains data from the National Land Survey of Finland Topographic Database 01/2014.